Radiology: Cardiothoracic Imaging

ORIGINAL RESEARCH

Utility of FDG PET and Cardiac MRI in Diagnosis and Monitoring of Immunosuppressive Treatment in Cardiac Sarcoidosis

Richard A. Coulden, MBBS • *Emer P. Sonnex, MPhil* • *Jonathan T. Abele, MD* • *Andrew M. Crean, MBBS, MPhil*

From the Department of Radiology and Diagnostic Imaging, University of Alberta Hospital, 8440 112 St NW, Edmonton, AB, Canada T6G 2B7 (R.A.C., E.P.S., J.T.A.); and Division of Cardiology, University of Ottawa Heart Institute, Ottawa, Ontario, Canada (A.M.C.). Received July 18, 2019; revision requested August 13; revision received April 2, 2020; accepted April 9. **Address correspondence to** R.A.C. (e-mail: *coulden@ualberta.ca*).

Conflicts of interest are listed at the end of this article.

See also commentary by Gutberlet in this issue.

Radiology: Cardiothoracic Imaging 2020; 2(4):e190140 • https://doi.org/10.1148/ryct.2020190140 • Content codes: CA MR

Purpose: To compare the contributions of cardiac MRI and PET in the diagnosis and management of cardiac sarcoidosis (CS), with particular reference to quantitative measures.

Materials and Methods: This is a retrospective, observational study of 31 patients (mean age, 45.7 years) with proven extracardiac sarcoidosis and possible CS who were investigated with fluorine 18 fluorodeoxyglucose (FDG) PET/CT and cardiac MRI. Patients were treated at physicians' discretion with repeat combined imaging after an interval of 102–770 days (median, 228 days).

Results: Significant myocardial FDG uptake was shown on visit 1 (myocardial maximum standardized uptake value [SUV_{max}] > 3.6) in 17 of 22 patients who were subsequently treated. Myocardial SUV_{max} decreased at follow-up (6.5 to 4.0; $P < .01$) and was matched by significant decreases in FDG-avid lung and mediastinal node disease. A volumetric measure of myocardium above a threshold SUV (cardiac metabolic volume) decreased from a mean of 42.5 to a mean of 4.1 ($P < .001$). This was associated with significant improvement in the left ventricular ejection fraction (LVEF) (45.8 increasing to 50.9; $P < .031$). There was no change in volume of late gadolinium enhancement at treatment. Patients who were untreated showed no change in any FDG PET or cardiac MRI parameter.

Conclusion: Myocardial FDG uptake in patients suspected of having CS is presumed to represent active inflammation. When treated with corticosteroids, this resolved or regressed at follow-up, with an improvement in LVEF and FDG-avid thoracic disease. Patients who were untreated showed no change in any parameter. Quantification of FDG-avid myocardium using cardiac metabolic volume is proposed as a useful objective measure for assessing response to therapy.

Symptomatic cardiac sarcoidosis (CS) is suspected in only 3%–5% of patients with sarcoidosis but is found at autopsy in 20%–30% of patients with sarcoidosis (1). Deaths due to CS represent 13%–25% of all sarcoidosis-related deaths in the United States (2,3) and represent up to 85% of all sarcoidosis-related deaths in Japan (3,4). As endomyocardial biopsy has a poor sensitivity for confirming CS (5), diagnosis is typically made using clinical criteria. The most referenced criteria come from the Japanese Ministry of Health and Welfare (JMHW) (6,7) and the Heart Rhythm Society (HRS) (8). Both include imaging findings from fluorine 18 fluorodeoxyglucose (FDG) PET and cardiac MRI; however, each examines a different aspect of the disease process. Late gadolinium enhancement (LGE) on cardiac MR images is believed to represent myocardial fibrosis or scarring (9), whereas abnormal myocardial FDG uptake on PET images represents active inflammation (10). The diagnosis of CS might therefore be enhanced when these techniques are combined. Additionally, authors generally describe the presence or absence of myocardial FDG uptake at PET without formal quantification of extent. The goal of this study was to compare the contributions of cardiac MRI and PET in the diagnosis and management of CS with particular reference to quantitative measures and clinical diagnostic criteria. Although not a primary objective, we also compared the impact of combined imaging on the diagnosis of CS using clinical criteria.

Materials and Methods

Study Population

This was a retrospective, observational study of patients suspected of having CS referred for imaging between August 2012 and May 2018. Patients were identified from our institutional CS imaging registry, which has approval from the institutional review board. The need for informed consent was waived, and a full chart review was not required. All patients had evidence of extracardiac sarcoidosis, either from biopsy results or from classic lung CT appearances. No patient had been shown to have CS at endomyocardial biopsy.

Eligibility Criteria

Patients were included if they had attended for combined FDG PET/CT and cardiac MRI on two occasions and had not been treated with oral steroids or other immunosuppressants for at least 6 months before their first attendance.

Abbreviations

CS = cardiac sarcoidosis, ECG = electrocardiography, FDG = fluorine 18 fluorodeoxyglucose, HRS = Heart Rhythm Society, JMHW = Japanese Ministry of Health and Welfare, LGE = late gadolinium enhancement, LV = left ventricular, LVEF = LV ejection fraction, SD = standard deviation, SSFP = steady-state free precession, SUV_{max} = maximum standardized uptake value

Summary

Diagnosis of cardiac sarcoidosis benefits from the combined use of cardiac MRI and fluorine 18 fluorodeoxyglucose (FDG) PET; at follow-up imaging, response to treatment was best assessed using quantitative FDG PET, and late enhancement at cardiac MRI did not regress.

Key Points

- Fluorine 18 fluorodeoxyglucose (FDG)–avid myocardial volume decreased significantly in patients treated for cardiac sarcoidosis (CS) (44 mL to 4 mL; $P < .001$); treatment was associated with improved left ventricular ejection fraction at cardiac MRI (45.8 increasing to 50.9; $P < .031$) but was associated with no change in volume of myocardial late enhancement.
- There was no change in any FDG PET or cardiac MRI parameter in the untreated group of patients presumed to have CS.

FDG PET/CT and cardiac MRI were performed on the same day wherever possible. Patients with a delay between PET/CT and cardiac MRI greater than 8 weeks on either visit were excluded. Patients in whom there was a change in immunosuppressive treatment status between PET/CT and cardiac MRI examinations (at either time point) were also excluded. Finally, patients who had or were suspected of having ischemic heart disease, valvular heart disease, insulin-dependent diabetes, or other inflammatory myocardial diseases were excluded to prevent false-positive myocardial FDG uptake. Of 90 patients in the registry eligible on the basis of two combined FDG PET and cardiac MRI examinations and a definite diagnosis of extracardiac sarcoidosis, 58 were excluded on the basis of the above criteria, with one being excluded for noncompliance with diet (Fig 1).

All patients were required to follow a strict low-carbohydrate diet the day before the examination (<3 g of carbohydrate over 24 hours) in combination with an overnight fast (11). Those who failed to adhere to either the diet or the fast had the PET component canceled and rebooked within 8 weeks. Patients with type 2 diabetes taking oral hypoglycemics stopped their hypoglycemic medication on the day of the low-carbohydrate diet and on the day of the examination and had to be diet and overnight-fast compliant.

All cases were reviewed independently by a cardiothoracic radiologist (R.A.C.) and an imaging cardiologist (A.M.C.) with expertise in PET and MRI (R.A.C., 30 years of experience in cardiac MRI and 18 years of experience in cardiac PET; A.M.C., 18 years of experience in cardiac MRI and 17 years of experience in cardiac PET). The clinical diagnosis of CS was based on criteria from the JMHW (7) and the HRS (8).

FDG PET/CT Imaging

Patient blood sugar levels were measured before injection of FDG, and a serum glucose level below 7 mmol/L was required. Radiotracer was given according to body weight (5.18 MBq/kg), with all PET/CT examinations being performed an hour later (Gemini TF; Philips, Eindhoven, the Netherlands). CT images were acquired from the neck to mid-abdomen during quiet breathing (0.5 second per rotation, 100-mAs tube current, and 120-kVp tube voltage). PET images were acquired with three to four bed positions (50% overlap) covering the same range, with 1 minute per bed position. Both data sets were reconstructed in 3-mm-thick slices with 50% overlap. PET data were acquired in three-dimensional mode and were iteratively reconstructed using CT-based attenuation correction.

Cardiac MRI

All examinations were performed with a 1.5-T scanner (Aera; Siemens Medical Systems, Erlangen, Germany) with a 32-channel phased-array coil. Steady-state free precession (SSFP) cine images were acquired in three long-axis planes (8-mm slice thickness; 25 phases; retrospective gating). T2-weighted short-tau inversion recovery images (8-mm slice thickness) were acquired at three short-axis locations (base apical, mid-apical, and periapical).

Intravenous gadolinium-based contrast material was then administered (0.2 mmol per kilogram of body weight gadopentetate dimeglumine), and short-axis cine SSFP imaging (8-mm thickness; 25% gap) was performed through the ventricles for assessment of biventricular ventricular function. At 10 minutes following contrast material administration, LGE imaging was performed in short and long axes using a phase-sensitive inversion recovery sequence, matching the cine SSFP slice thickness and positions. Inversion time was determined on an individual patient basis to obtain optimal nulling of the unenhanced myocardial signal (typically 270–330 msec).

FDG PET/CT Analysis

All PET/CT data were transferred to an offline workstation for analysis using three-dimensional fusion software (Oasis; Segami, Columbia, Md).

Active extracardiac sarcoid involvement was considered present if there was abnormal intra- or extrathoracic nodal-tracer uptake, abnormal pulmonary parenchymal-tracer uptake, or abnormal tracer activity in the liver or spleen. Maximum standardized uptake value (SUV_{max}) thresholds were used to define abnormality as per Wang et al (12) (for nodes, an $SUV_{max} > 2.5$ and/or >1.0 higher than blood-pool SUV_{max}; for pulmonary nodules or nodular consolidation, an $SUV_{max} > 1.5$ and/or >0.5 higher than background normal lung; and for liver or spleen, an $SUV_{max} > 5.0$).

The SUV_{max} of the mediastinal blood pool was estimated using a 30-mm spherical region of interest in the right atrium. The threshold for identifying abnormal myocardial FDG uptake was based on a published historical population of oncology patients with no evidence of cardiac disease, who had undergone the same imaging protocol on the same imaging system with the same dietary and fasting preparation. Myocardial SUV_{max} in this diet-prepared group was 1.8 ± 0.9 standard deviation (SD), giving a threshold for abnormal myocardium in this study population of

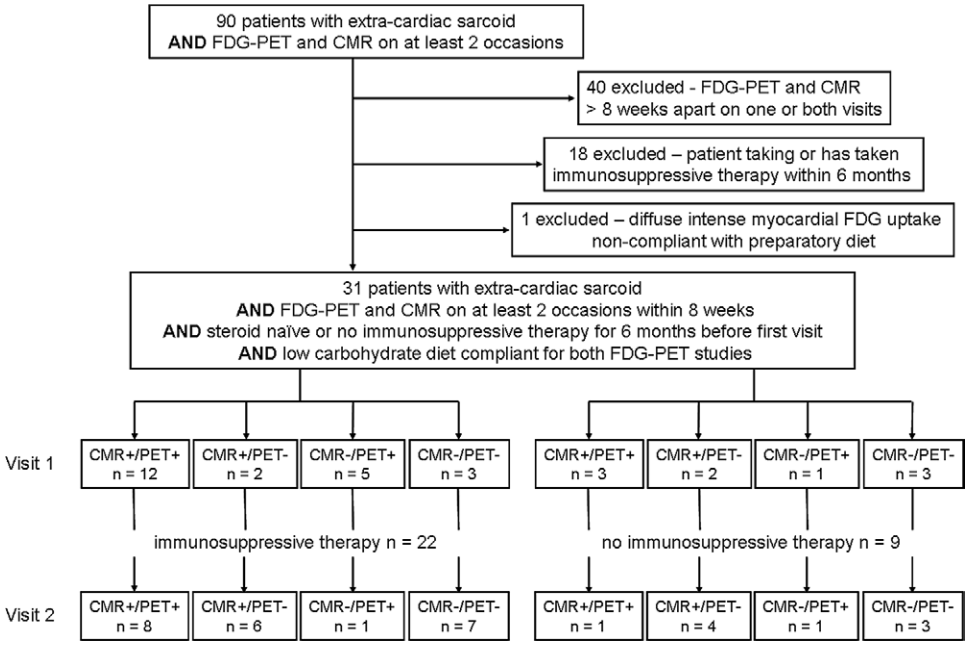

Figure 1: Flowchart details selection criteria for the study cohort and fluorine 18 fluorodeoxyglucose (FDG) PET and cardiac MRI late gadolinium enhancement (LGE) results in treated and untreated groups at initial and follow-up studies. CMR = cardiac MRI.

SUV_{max} greater than 3.6 (mean + 2 SDs) (11). This was further characterized as intense if SUV_{max} was greater than 4.5 (mean +3 SDs). Any patient found to have diffuse intense myocardial uptake was excluded because of presumed failure of suppression of normal physiologic glucose metabolism (13).

The volume of abnormal myocardial FDG uptake was quantified using dedicated software (Metavol; Hokkaido University, Sapporo, Japan). Cardiac metabolic volume was calculated using a threshold SUV_{max} greater than 3.6. Having identified sites of abnormal cardiac activity, the distribution of FDG-avid myocardium uptake was mapped to a modified American Heart Association model for left ventricular (LV) segmentation designed to include the right ventricle (14). All PET measurements for both examinations were performed by the same observer (A.M.C.). To assess intraobserver variability in the measurement of cardiac metabolic volume, measurements for the initial FDG PET/CT examination were repeated.

Cardiac MRI Analysis

All cardiac MRI data were transferred to an offline workstation for visual assessment and analysis (cvi42; Circle Cardiovascular Imaging, Calgary, Canada). LV and right ventricular volumes and ejection fractions were derived using manual planimetry of short-axis SSFP slices (15). The presence of myocardial edema was assessed visually from T2-weighted short-tau inversion recovery images and postcontrast cine SSFP images, and myocardial LGE was quantified from the magnitude images of the short-axis phase-sensitive inversion recovery stack (16,17). A region of interest drawn in remote normal myocardium on each magnitude slice was used to define the signal threshold for calculation of LGE volume (mean of normal myocardium + 5 SDs) (18). As LGE in the right ventricle was also included in the volume calculation, LGE volume is expressed in milliliters rather than as a percentage of the LV myocardium, as in other publications (19). As with abnormal myocardial FDG uptake, the distribution of LGE was mapped to the model of ventricular segmentation. All measurements for both examinations were performed by the same observer (R.A.C.). To assess intraobserver variability in the assessment of LGE volume, this component of the analysis was repeated for all initial cardiac MRI examinations.

Statistical Analysis

Categorical data are reported as frequencies and percentages. Continuous data were assessed for normal distribution using the Shapiro-Wilk test and expressed as mean ± SD. Paired Student *t* tests were used for paired comparisons of normally distributed data (ventricular function and volumes). SUV_{max} values for blood pool, myocardium, and so forth, and LGE and cardiac metabolic volumes were not normally distributed. The Wilcoxon signed rank test was used to compare these paired data sets. Values, however, are given as mean ± SD, as median values on visit 2 were often zero. Unpaired data (SUV_{max} values, LGE, and cardiac metabolic volumes between treated and untreated groups at initial PET/CT and cardiac MRI) were not normally distributed and were compared using the Mann-Whitney *U* test. Intraobserver variability in measurement of cardiac metabolic volume and LGE volumes were assessed by Bland-Altman analysis and are expressed as the bias ± 2 SDs for limits of agreement. A *P* value less than .05 was considered to indicate a significant difference. Statistical analyses were performed using MedCalc, version 12.1.3 (MedCalc Software, Mariakerke, Belgium).

Results

Thirty-one patients (24 men, seven women; mean age of men, 46 years ± 14.5; mean age of women, 46 years ± 15.4) underwent cardiac MRI and FDG PET on two occasions separated by a median of 228 days. FDG PET was performed in the morning, and cardiac MRI was performed in the afternoon. Both examinations were completed the same day in 50 of 62 combined studies. Intervals between PET and cardiac MRI for the remaining 12 attendances were less than 1 week (four patients), 1–4 weeks (two patients), and 5–8 weeks (six patients). None of these patients had a change in immunosuppressive therapy between undergoing PET and cardiac MRI.

Patient demographics at first attendance are summarized in Table 1.

Table 1: Patient Characteristics at Baseline

Parameter	No-Treatment Group	Treatment Group
No. of patients	9	22
Age (y)*	50 ± 6.2	48 ± 11.1
Men*	56 ± 6.8	47 ± 10.3
Women*	57 ± 5.6	52 ± 15.5
No. of men	6 (67)	18 (82)
Symptoms	4 (44)	15 (68)
Palpitations	4 (44)	11 (50)
Breathlessness	…	3 (14)
Chest pain	…	3 (14)
No. with biopsy-proven extracardiac sarcoid	7 (78)	18 (82)
No. with pulmonary sarcoid at CT	2 (22)	4 (18)
No. with abnormal ECG	4 (44)	20 (91)
Left-bundle-branch block	…	3 (14)
Right-bundle-branch block†	…	1 (5)
Intraventricular conduction delay	…	2 (9)
Axis deviation†	…	1 (5)
Abnormal Q waves†	…	…
First-degree heart block	1 (11)	…
Second- or third-degree heart block‡	1 (11)	4 (18)
Frequent PVCs or ventricular tachycardia†	…	3 (14)
Atrial fibrillation	1 (11)	3 (14)
Resting tachycardia (>100 beats/min)	1 (11)	3 (14)
Patients suspected of having CS on the basis of previous cardiac MRI findings	2 (22)	6 (27)
Patients suspected of having CS on the basis of symptoms and ECG findings	7 (78)	20 (73)

Note.—Unless otherwise indicated, data are number of patients with percentages in parentheses.
CS = cardiac sarcoidosis, ECG = electrocardiogram, PVCs = premature ventricular contractions.
* Data are means ± standard deviations.
† Minor criterion as per Japanese Ministry of Health and Welfare guidelines.
‡ Major criterion as per Japanese Ministry of Health and Welfare guidelines.

Cardiac Findings at FDG PET and Cardiac MRI: Visit 1

Abnormal myocardial FDG uptake (SUV_{max} > 3.6) was seen in 21 patients; 14 of these were referred for imaging on the basis of electrocardiographic (ECG) and echocardiographic criteria, and seven were referred for LGE results suspicious for sarcoidosis at a historical cardiac MRI. In 18 of these patients, myocardial SUV_{max} was greater than 4.5 (ie, focal intense), and in the three in whom this threshold was not met (ie, focal), LV function was impaired. In one of these, the site of myocardial FDG PET uptake was also matched by LGE.

At T2-weighted imaging and postcontrast cine SSFP, myocardial edema and/or hyperemia was seen in four of 31 cases (13%). In all four, this was matched by LGE and focal intense myocardial FDG uptake. Seventeen patients suspected of having active CS by myocardial FDG uptake had no edema at MRI. Nineteen patients showed a nonischemic pattern of myocardial enhancement (61%). Seven of these had basal septal thinning, and 15 showed LV impairment (LV ejection fraction [LVEF] < 50% using JMWH criteria). Twelve showed more severe LV impairment (LVEF < 40% using HRS criteria).

Intraobserver variability for measurement of LGE volume was low (bias, 0.7 mL ± 3.2) and was similar to previous published values (20). Intraobserver variability for measurement of cardiac metabolic volume was extremely low (bias, 0.0 mL ± 0.7).

Extracardiac Findings at FDG PET and Cardiac MRI: Visit 1

Abnormal extracardiac FDG avidity was seen in 29 of 31 patients (94%); it was seen in the lung parenchyma in 25 (81%), in thoracic nodal groups in 25 (81%), and in an extrathoracic location (cervical, axillary, or abdominal nodes, the spleen, the liver, or a combination) in 18 (58%). Two patients showed abnormal myocardial FDG uptake in the absence of sarcoid-related tracer uptake elsewhere. Both were associated with LGE on cardiac MR images and both had a history of remote treatment with corticosteroids for suspected CS on the basis of nonischemic LGE at a prior cardiac MRI.

Concordance between Cardiac MRI LGE and Myocardial FDG for Presence or Absence of Cardiac Involvement: Visit 1

There were 15 of 31 cases in which both LGE and abnormal myocardial FDG uptake were present and six in which there was neither (concordance 68%). In six patients, there was abnormal myocardial FDG uptake with no detectable LGE, and in four there was LGE without abnormal myocardial FDG (Figs 1, 2). Cardiac MRI and PET results were discordant in 32%. When FDG PET/CT and cardiac MRI findings were combined with ECG abnormalities, 14 patients (45%) met modified JMHW criteria for the diagnosis of CS and 20 (64%) met HRS criteria. Eight patients met neither (Table 2). Three JMHW-positive patients were HRS-negative

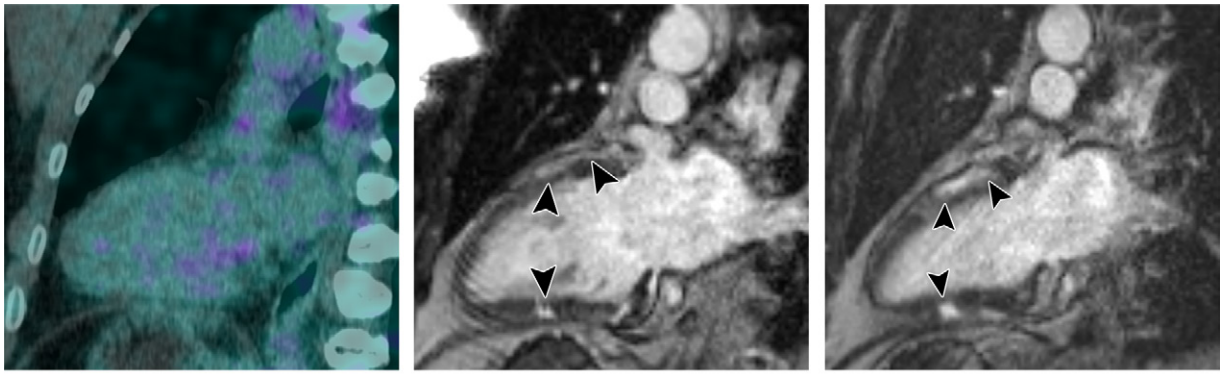

a. b. c.

Figure 2: Images in a 50-year-old man with stage 2 sarcoidosis for 12 months develops resting tachycardia (100+ beats per minute). There is no myocardial tracer uptake on the **(a)** two-chamber fused PET/CT image, despite **(b)** multifocal nonischemic late gadolinium enhancement (LGE) in the anterior and inferior wall on the cardiac MR image (black arrowheads). The patient is not treated with corticosteroids and returns 6 months later. **(c)** There is still no myocardial fluorine 18 fluorodeoxyglucose uptake, although LGE is a little more prominent. There was no change in biventricular function or volumes (patient 7, Table 2).

because of the requirement for biopsy confirmation of extracardiac sarcoidosis by HRS criteria. JMHW criteria require either biopsy or clinical imaging, in keeping with extracardiac disease. Had cardiac MRI been used alone, only eight cases would have met JMHW criteria, and 20 would have met HRS criteria. Using FDG PET alone, only one case would have been JMHW-positive, and 17 cases would have been HRS-positive.

Findings at FDG PET and Cardiac MRI: Visit 2

Thirty-one follow-up cardiac MRI and PET studies were performed 102–770 days (median, 228 days) after the initial combined study. Twenty-two of 31 patients (68%) were treated with oral prednisone between visits, seven having concomitant treatment with methotrexate or mycophenolate. Although there was no standard regimen for immunosuppression, all patients were initiated with a moderate-to-high dose of prednisone (30–50 mg per day), tapering to a maintenance dose of 5–10 mg per day. Treatment duration varied from 3 to 15 months, with all patients being re-examined while still taking immunosuppressants or within 3 months of stopping. In the two instances in which the interval between visits exceeded 12 months, one was for a patient not receiving treatment (770 days) and the other was for a patient who had been taking steroids for 15 months (497 days).

As an observational study, the decision to treat was made by the referring physician and the patient. Despite five patients meeting JMHW and/or HRS clinical criteria for CS, they were not treated. Three of these had active cardiac CS as determined with FDG PET. The reason for not treating is unknown. Four patients who met neither set of criteria were treated.

There were significant reductions in myocardial SUV_{max} (6.5 ± 3.1, decreasing to 4.0 ± 2.5; $P < .01$) and cardiac metabolic volume (42.5 mL ± 65.1, falling to 4.1 mL ± 10.5; $P < .001$). The decrease in abnormal cardiac metabolic activity was matched by an improvement in LVEF (45.8 ± 12.7, increasing to 50.9 ± 8.7; $P < .031$) and a reduction in LV end-systolic volume. Right ventricular end-systolic volume also decreased significantly with a trend toward improved right ventricular ejection fraction. The fall in myocardial SUV_{max} was accompanied by a significant reduction in FDG-avid lung and mediastinal node disease (Fig 3). Despite the improvement in LVEF in the treated group, there was no change in the volume of LGE (Table 3). Unfortunately, neither initial myocardial SUV_{max} nor the size of the decrease in cardiac metabolic volume predicted improvement in LVEF. Whether this lack of correlation is genuine or has been masked by relatively short follow-up interval remains unclear.

Comparing treated and nontreated groups at visit 1, there was no statistical difference in SUV_{max} values in mediastinal node or lung disease. Myocardial SUV_{max}, however, was significantly lower in the nontreated group ($P = .03$), presumably reflecting less severe cardiac involvement. Cardiac metabolic volume and LGE volume in the nontreated group were also lower, but this did not reach statistical significance ($P = .095$ and $P = .217$, respectively). In the untreated group, there was no reduction in myocardial SUV_{max}, cardiac metabolic volume, or volume of LGE. There was also no change in ventricular function or volumes.

Figure 4 shows the distribution of abnormal myocardial FDG uptake and LGE on initial and follow-up visits. This confirms previous reports that CS has a predilection for the proximal anterior wall and proximal septum and the proximal and mid-inferior and mid-inferolateral walls (21). The LV apex and periapical region were virtually spared. Although sites of abnormal myocardial FDG uptake were frequently matched by LGE on the initial study, FDG uptake was considerably more extensive. Unmatched FDG uptake was particularly common in the inferior and inferolateral wall of the LV, sites often believed to be nonsuppressed physiologic myocardial uptake. Regression or resolution of these sites with treatment, matched by improvement in extrathoracic disease and increased LVEF, suggests this genuinely represents disease (Fig 5). In the untreated group, inferior and inferolateral FDG uptake was unchanged or increased between visits. When present, LGE was frequently patchy and at the mid wall as described in CS, but there was no definitive pattern. During the follow-up period of this study, LGE did not resolve.

Table 2: FDG PET/CT and Cardiac MRI Findings on Visit 1 and Correlation with JMHW and HRS Criteria

		Extracardiac FDG				JMHW Major Criteria				JMHW Minor Criteria			
Patient No.	Extracardiac Sarcoidosis	FDG-Avid Thoracic Nodes, 1 = Y	FDG-Avid Lung Disease, 1 = Y	FDG-Avid Extrathoracic Disease, 1 = Y	Pattern of Abnormal Myocardial FDG Uptake	Cardiac FDG SUV$_{max}$ > 3.6, 2 = Y*	Basal Septal Thinning, 2 = Y*	VT or Advanced AVB, 2 = Y*	Cardiac MR LVEF < 50%, 2 = Y†	Abnormal ECG, 1 = Y	Cardiac MRI LGE, 1 = Y	JMWH+, 1 = Y	HRS+, 1 = Y
1	1	1	1	1	0	0	0	0	63	0	1	0	1
2	1	1	1	1	0	0	0	0	55	0	0	0	0
3	1	1	1	1	0	0	0	0	46	0	0	0	0
4	1	0	0	0	Focal	2	0	0	49	0	1	1	1
5	1	1	1	0	Focal intense	2	0	0	44	0	1	1	1
6	0	0	1	0	Focal intense	2	0	0	65	0	0	0	0
7	1	1	1	1	0	0	0	0	64	0	1	0	1
8	0	0	1	0	0	0	0	0	56	0	0	0	0
9	1	1	1	0	Focal intense on diffuse	2	0	2	62	0	1	1	1
10	1	1	1	1	0	0	0	0	65	0	0	0	0
11	0	1	0	0	0	0	0	0	39	0	0	0	0
12	1	1	0	1	Focal intense	2	2	0	24	0	1	1	1
13	0	1	1	1	Focal intense	2	2	2	39	0	1	1	0
14	0	1	1	0	Focal intense	2	0	2	49	0	1	1	0
15	1	1	1	1	Focal intense	2	0	0	53	0	1	0	1
16	1	1	1	1	0	0	2	0	47	1	1	1	1
17	1	1	0	0	Focal intense	2	0	0	60	1	0	0	1
18	1	1	1	1	Focal intense on diffuse	2	2	2	43	0	1	1	1
19	1	1	1	1	0	0	0	0	43	0	0	0	0
20	1	0	0	0	Focal intense on diffuse	2	0	0	23	0	1	1	1
21	1	1	1	1	Focal intense on diffuse	2	2	0	47	0	1	1	1
22	0	1	1	0	Focal intense	2	0	0	52	0	0	0	0
23	0	1	0	1	Focal	2	0	0	27	0	0	1	0
24	1	1	1	1	Focal intense	2	0	0	56	1	0	0	1
25	1	1	1	0	0	0	0	0	30	0	1	0	1
26	1	1	1	1	Focal intense	2	2	2	55	0	1	1	1
27	1	0	1	0	Focal intense	2	0	0	63	0	1	0	1

Table 2 (*continues*)

Table 2: FDG PET/CT and Cardiac MRI Findings on Visit 1 and Correlation with JMHW and HRS Criteria

Patient No.	Extracardiac Sarcoidosis	Extracardiac FDG				JMHW Major Criteria				JMHW Minor Criteria			HRS
		FDG-Avid Thoracic Nodes, 1 = Y	FDG-Avid Lung Disease, 1 = Y	FDG-Avid Extrathoracic Disease, 1 = Y	Pattern of Abnormal Myocardial FDG Uptake	Cardiac FDG $SUV_{max} > 3.6$, 2 = Y*	Basal Septal Thinning, 2 = Y*	VT or Advanced AVB, 2 = Y*	Cardiac MR LVEF < 50%, 2 = Y†	Abnormal ECG, 1 = Y	Cardiac MRI LGE, 1 = Y	JMWH+, 1 = Y	HRS+, 1 = Y
28	1	1	1	1	Focal intense on diffuse	2	0	0	62	0	0	0	1
29	1	0	1	1	Focal	2	0	0	34	0	1	1	1
30	1	1	1	1	Focal intense	2	2	0	40	0	1	1	1
31	1	1	1	0	Focal intense	2	0	0	63	0	1	0	1

Note.—Patients 1–9 were not treated following visit 1; patients 10–31 were treated with immunosuppressants. Extracardiac sarcoidosis is proven with biopsy = 1; extracardiac sarcoidosis is proven with clinical imaging = 0. Pattern of myocardial FDG uptake: focal = $SUV_{max} > 3.6 < 4.5$, focal intense = $SUV_{max} > 4.5$. AVB = atrioventricular block, ECG = electrocardiogram, FDG = fluorodeoxyglucose, HRS = Heart Rhythm Society (positive if biopsy-proven extracardiac sarcoid and any HRS criteria), JMHW = Japanese Ministry of Health and Welfare (positive if two major criteria or one major and two minor), LVEF = left ventricular ejection fraction, SUV_{max} = myocardial maximum standardized uptake value, VT = ventricular tachycardia, Y = yes, + = positive.

* HRS criteria.

† HRS criteria: unexplained LVEF less than 40% rather than less than 50% for JMHW.

Discussion

Our study, using both modalities nearly simultaneously, has shown myocardial FDG to be a more sensitive marker for active myocardial disease than the presence of either edema at T2-weighted imaging or LGE. When present, myocardial FDG uptake virtually always regressed or resolved with treatment, but neither the intensity of uptake nor the metabolic volume were good predictors of improvement in LVEF. Coincident regions of FDG uptake and LGE were common but were not the rule; choosing to perform either PET or cardiac MRI alone could underestimate the extent of disease and the need for treatment. In the treatment group, LVEF improved by more than 5% in eight patients. Although five of these demonstrated a combined pattern of LGE and myocardial FDG uptake, one had myocardial FDG uptake alone, and two had LGE alone. In both LGE cases, there was focal myocardial FDG uptake just below our threshold for abnormality ($SUV_{max} > 3.6$).

The use of JMHW or HRS criteria is equally problematic in guiding treatment. Five patients meeting one or other criteria were not treated, with only one of these deteriorating at follow-up. Eighteen of 22 patients in the treatment group met clinical criteria, but only seven of these showed improvement in LVEF. This mirrors the experience of others using the same criteria and underlines the need for better reference standards (22).

In this study, response to therapy was more readily assessed with PET than with cardiac MRI. Both myocardial SUV_{max} values and cardiac metabolic volume decreased with treatment, and this was frequently accompanied by matched decreases in metabolic activity in nodal and lung disease. The most sensitive indicator of the myocardial response to treatment was cardiac metabolic volume. Although previous investigators have suggested that cardiac MRI can be used for monitoring the treatment response in CS (23), we have found it unhelpful. Myocardial edema on T2-weighted images was uncommon and, where present, was always matched by delayed enhancement (four of 19 patients with LGE [21%]). This is similar to previously published data in which five of 34 patients with LGE showed edema on T2-weighted images (24). LGE in CS is generally considered to be a marker of scarring or fibrosis, and, as anticipated, the volume of LGE did not change at follow-up.

Three patterns of myocardial involvement were seen in this cohort: myocardial FDG uptake alone, matched myocardial FDG uptake and LGE, and LGE alone. The pathologic basis for these patterns remains to be confirmed, but if CS in the myocardium is similar to that described in the lung, these imaging patterns can be explained (25). The earliest phase of CS is believed to be an inflammatory myocarditis, indistinguishable from a lymphocytic myocarditis (21). This might correspond to unmatched myocardial FDG uptake. In the lung, this can resolve spontaneously, but it is not known whether this also occurs in the heart. If so, it may not always need to be treated. As others have found (26), the most common appearance in this study was matched myocardial FDG uptake and LGE, representing the active granulomatous phase. The late fibrotic phase, well recognized in sarcoid lung disease,

contains few inflammatory cells and is presumed responsible for unmatched myocardial LGE. In the absence of FDG-avid myocardium, response to immunosuppression is theoretically less likely.

For FDG PET to be of value in identifying CS, physiologic myocardial FDG uptake must be suppressed. There is no consensus as to the best technique for doing this, but most investigators advocate a preparatory low-carbohydrate diet and overnight fast (27,28). There is no agreement that failure to comply with the diet should lead to cancellation of the study. Published failure rates for myocardial suppression are high (29). In this study, patients found to be noncompliant with strict dietary instructions (as judged by food questionnaire responses on the day of imaging) had their examinations canceled and rebooked. We canceled and rebooked six of 31 patient examinations (19%) and had one failed suppression that was excluded as per Figure 1. Had we not canceled and rebooked, our rate of failed myocardial suppression may have been similar to those of published series.

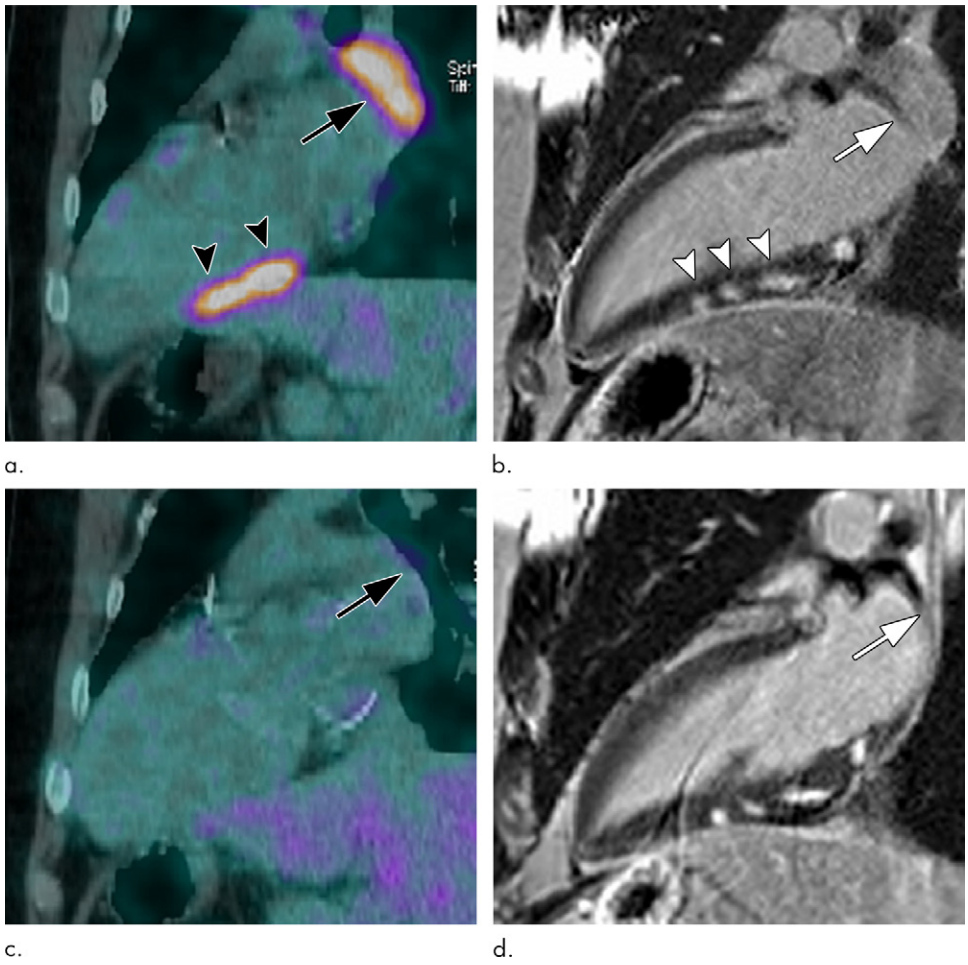

Figure 3: Images in a 35-year-old man with third-degree heart block and stage 1 sarcoidosis. **(a)** Fluorine 18 fluorodeoxyglucose (FDG)–avid myocardium (maximum standardized uptake value [SUV_{max}] = 7.6) in the inferior wall of the left ventricle on a two-chamber fused PET/CT image (black arrowheads). **(b)** This matches late gadolinium enhancement (LGE) on cardiac MR image but is more extensive (white arrowheads). **(a)** A large FDG-avid subcarinal lymph node (SUV_{max} = 6.1) (black arrow). **(a, c)** At follow-up after 6 months of oral corticosteroids, myocardial FDG uptake has resolved, as has uptake in the large subcarinal node (black arrow). **(b, d)** There is little change in LGE. Left ventricular function is mildly impaired on both studies. **(b, d)** A large subcarinal lymph node (white arrow) has resolved at MRI (patient 14, Table 2).

Limitations

This is a single-center, retrospective observational study based on registry-collected data. To identify a coherent patient group with stringent inclusion criteria, a large number of cases had to be excluded. Despite resulting small numbers, our cohort is similar in size to those of other published series in which only FDG PET or cardiac MRI were used (23,30,31), and the impact of treatment on cardiac and extracardiac FDG uptake and LV remodeling and function was significant.

We did not perform a resting nuclear perfusion examination as part of our study protocol. The rationale was that cardiac MRI can be used to accurately identify abnormalities that cause resting defects on nuclear perfusion (ie, hibernating myocardium, myocardial infiltration, and scarring [LGE]) (32–34) and, as such, could replace the resting nuclear perfusion scan. In a previous study comparing LGE with resting nuclear perfusion in CS (35), a third of segments showing nonischemic LGE had normal resting perfusion. In all segments without LGE, resting perfusion was also normal. More recently, the same has been shown in inflammatory cardiomyopathies in which nuclear perfusion was compared with PET/CT or PET/MRI (33). Although there remains a risk that focal FDG uptake in resting ischemia might be misinterpreted as CS, in this cohort, patients who had or were suspected of having ischemia were excluded.

Although using an SUV_{max} threshold discriminates between abnormal and physiologic myocardial tracer uptake in the majority of cases, there is a risk of missing low-grade active disease. The overlap between physiologic and low-grade pathologic uptake means there is no threshold that can be used to identify all patients with active CS. Whether missing low-grade CS is important or not remains unclear.

Our cardiac MRI study protocol did not include native T1 mapping. This has recently been shown as a way to discriminate between patients with CS and control patients without CS and has potential for assessing disease activity (36). This sequence, however, was not available to us in the early years of data collection.

This study combined concurrent cardiac MRI and PET/CT for the diagnosis and management of CS. Logistically,

Table 3: Changes between Visits for Ventricular Parameters, SUV_{max}, and LGE for Treated and Untreated Groups

	Treatment Group (n = 22)			No-Treatment Group (n = 9)		
Parameter	Visit 1	Visit 2	*P* Value	Visit 1	Visit 2	*P* Value
LVEDV (mL)	186.4 ± 67.0	179.7 ± 57.3	.373	155.8 ± 37.7	158.9 ± 39.3	.704
LVESV (mL)	105.6 ± 59.6	92.0 ± 45.7	.057	69.1 ± 22.2	67.0 ± 24.4	.798
LVEF%	45.8 ± 12.6	50.8 ± 8.7	.031	56.0 ± 8.2	58.5 ± 7.7	.478
RVEDV (mL)	169.7 ± 42.1	162.9 ± 39.5	.323	157.8 ± 46.1	164.3 ± 53.7	.573
RVESV (mL)	92.2 ± 37.2	80.7 ± 25.6	.040	77.8 ± 28.5	82.4 ± 34.1	.611
RVEF (%)	46.6 ± 11.3	50.8 ± 6.5	.089	51.6 ± 9.5	50.8 ± 12.1	.792
Myocardial SUV_{max}	6.5 ± 3.1	4.0 ± 2.5	.002	3.9 ± 1.7	3.5 ± 2.3	.426
CMV in mL (threshold SUV > 3.6)	42.5 ± 65.5	4.1 ± 10.5	.001	6.0 ± 15.5	19.9 ± 59.3	.875
Lung SUV_{max}	3.7 ± 2.8	2.1 ± 1.8	.008	2.6 ± 1.2	2.5 ± 1.7	.496
Mediastinal node SUV_{max}	5.4 ± 3.0	3.9 ± 2.9	.020	4.4 ± 2.8	5.0 ± 4.5	.652
Blood pool SUV_{max}	2.4 ± 0.3	2.3 ± 0.4	.41	2.1 ± 0.2	2.0 ± 0.3	.688
Spleen SUV_{max}	3.5 ± 1.7	2.7 ± 0.7	.105	3.0 ± 1.6	3.6 ± 2.6	.148
Liver SUV_{max}	3.8 ± 0.6	3.8 ± 0.6	.639	3.3 ± 0.4	3.4 ± 0.5	.469
LGE volume, mean + 5 SDs (mL)	7.7 ± 10.6	6.3 ± 7.9	.080	2.0 ± 2.9	1.3 ± 1.8	.313

Note.—Unless otherwise indicated, data are means ± standard deviations. CMV = cardiac metabolic volume, LGE = late gadolinium enhancement, LVEDV = left ventricular end-diastolic volume, LVEF = left ventricular ejection fraction, LVESV = left ventricular end-systolic volume, RVEDV = right ventricular end-diastolic volume, RVEF = right ventricular ejection fraction, RVESV = right ventricular end-systolic volume, SD = standard deviation, SUV_{max} = maximum standardized uptake value.

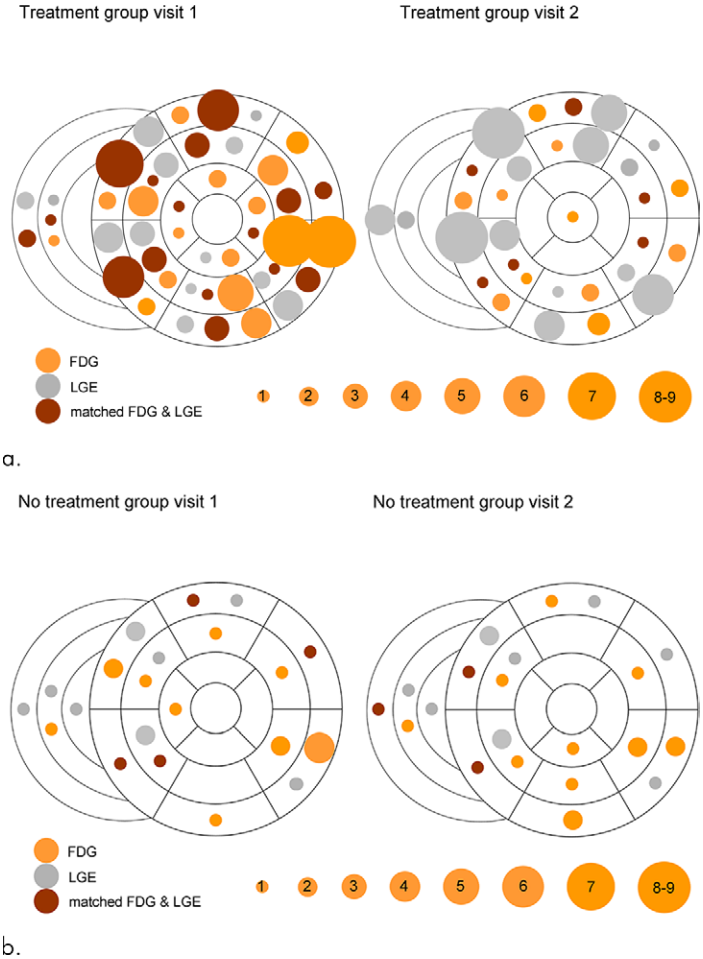

Figure 4: Plots of distribution of abnormal myocardial fluorine 18 fluorodeoxyglucose (FDG) uptake and late gadolinium enhancement (LGE) on initial and follow-up studies in the **(a)** treatment and **(b)** nontreatment groups. The color of the dots represents FDG uptake alone, matched FDG and LGE, and LGE alone in each segment. The size of the dot indicates the number of patients with that abnormality. In the treatment group, matched FDG and LGE on visit 1 becomes unmatched LGE on visit 2 in the majority of cases. There is little change in the untreated group.

this was complex, and, at times, one component or the other had to be canceled and rebooked. These difficulties are eliminated using PET/MRI, and there are theoretical advantages in inflammatory cardiomyopathies (26,33,37). Access to PET/MRI, however, is even more restricted than having PET/CT and cardiac MRI in the same institution. It has also yet to be shown that this technique has significant advantages over same-day examinations performed as we describe here.

Conclusion

CS has important prognostic implications for patients with established extracardiac sarcoidosis, and yet it may be difficult to detect using any single imaging modality. We have found same-day FDG PET/CT and cardiac MRI to be both practical and effective in the diagnosis and monitoring of CS. Using either technique alone creates a risk of missing treatable cardiac disease or treating disease that is inactive. For monitoring patients with CS, we have found cardiac metabolic volume at FDG PET to be the most useful parameter for guiding therapy.

Author contributions: Guarantor of integrity of entire study, R.T.C.; study concepts/study design or data acquisition or data analysis/interpretation, all authors; manuscript drafting or manuscript revision for important intellectual content, all authors; approval of final version of submitted manuscript, all authors; agrees to ensure any questions related to the work are appropriately resolved, all authors; literature research, all authors; clinical studies, R.A.C., E.P.S., J.T.A.; statistical analysis, R.A.C., A.M.C.; and manuscript editing, all authors.

Disclosures of Conflicts of Interest: R.A.C. disclosed no relevant relationships. **E.P.S.** disclosed no relevant relationships. **J.T.A.** disclosed no relevant relationships. **A.M.C.** disclosed no relevant relationships.

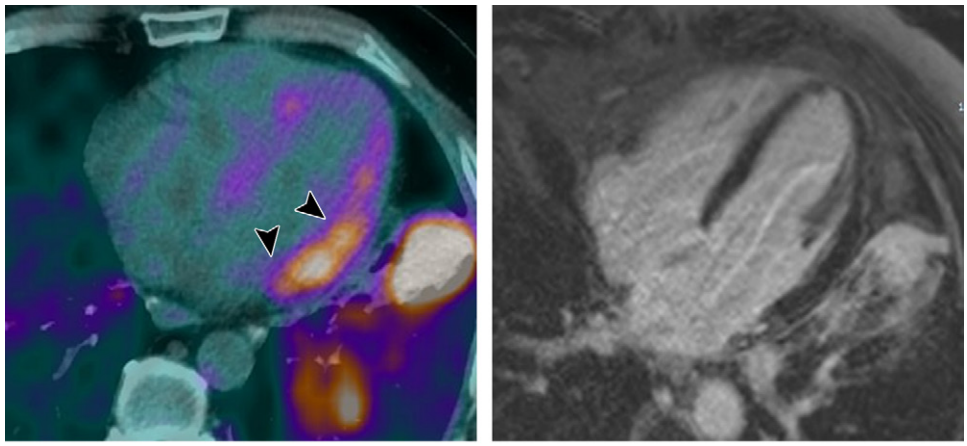

a. b.

Figure 5: Images in a 54-year-old man with stage 2 sarcoidosis for 2 years develops new right-bundle-branch block shown on an electrocardiogram. Myocardial fluorine 18 fluorodeoxyglucose (FDG) uptake (maximum standardized uptake value [SUV_{max}] = 4.6) without matching late gadolinium enhancement (LGE) is shown on the **(a)** four-chamber fused PET/CT image (black arrowheads) and **(b)** cardiac MR image. With normal left ventricular (LV) function, this patient does not meet Japanese Ministry of Health and Welfare criteria but does meet Heart Rhythm Society criteria. He is treated with corticosteroids for 6 months. Follow-up PET/CT and cardiac MR images show resolution of cardiac and extracardiac FDG uptake at all sites. LGE does not develop, and LV function is unchanged. Pulmonary parenchymal disease also partly regresses at MRI (patient 24, Table 2).

References

1. Silverman KJ, Hutchins GM, Bulkley BH. Cardiac sarcoid: a clinicopathologic study of 84 unselected patients with systemic sarcoidosis. Circulation 1978;58(6):1204–1211.
2. Roberts WC, McAllister HA Jr, Ferrans VJ. Sarcoidosis of the heart. A clinicopathologic study of 35 necropsy patients (group 1) and review of 78 previously described necropsy patients (group 11). Am J Med 1977;63(1):86–108.
3. Swigris JJ, Olson AL, Huie TJ, et al. Sarcoidosis-related mortality in the United States from 1988 to 2007. Am J Respir Crit Care Med 2011;183(11):1524–1530.
4. Yazaki Y, Isobe M, Hiroe M, et al. Prognostic determinants of long-term survival in Japanese patients with cardiac sarcoidosis treated with prednisone. Am J Cardiol 2001;88(9):1006–1010.
5. Uemura A, Morimoto S, Hiramitsu S, Kato Y, Ito T, Hishida H. Histologic diagnostic rate of cardiac sarcoidosis: evaluation of endomyocardial biopsies. Am Heart J 1999;138(2 Pt 1):299–302.
6. Hulten E, Aslam S, Osborne M, Abbasi S, Bittencourt MS, Blankstein R. Cardiac sarcoidosis-state of the art review. Cardiovasc Diagn Ther 2016;6(1):50–63.
7. Ohira H, Birnie DH, Pena E, et al. Comparison of (18)F-fluorodeoxyglucose positron emission tomography (FDG PET) and cardiac magnetic resonance (CMR) in corticosteroid-naive patients with conduction system disease due to cardiac sarcoidosis. Eur J Nucl Med Mol Imaging 2016;43(2):259–269.
8. Birnie DH, Sauer WH, Bogun F, et al. HRS expert consensus statement on the diagnosis and management of arrhythmias associated with cardiac sarcoidosis. Heart Rhythm 2014;11(7):1305–1323.
9. Olimulder MA, Galjee MA, van Es J, Wagenaar LJ, von Birgelen C. Contrast-enhancement cardiac magnetic resonance imaging beyond the scope of viability. Neth Heart J 2011;19(5):236–245.
10. Braun JJ, Kessler R, Constantinesco A, Imperiale A. 18F-FDG PET/CT in sarcoidosis management: review and report of 20 cases. Eur J Nucl Med Mol Imaging 2008;35(8):1537–1543.
11. Coulden R, Chung P, Sonnex E, Ibrahim Q, Maguire C, Abele J. Suppression of myocardial 18F-FDG uptake with a preparatory "Atkins-style" low-carbohydrate diet. Eur Radiol 2012;22(10):2221–2228.
12. Wang Y, Chiu E, Rosenberg J, Gambhir SS. Standardized uptake value atlas: characterization of physiological 2-deoxy-2-[18F]fluoro-D-glucose uptake in normal tissues. Mol Imaging Biol 2007;9(2):83–90.
13. Ishida Y, Yoshinaga K, Miyagawa M, et al. Recommendations for (18) F-fluorodeoxyglucose positron emission tomography imaging for cardiac sarcoidosis: Japanese Society of Nuclear Cardiology recommendations. Ann Nucl Med 2014;28(4):393–403.
14. Bangalore S, Yao SS, Chaudhry FA. Role of right ventricular wall motion abnormalities in risk stratification and prognosis of patients referred for stress echocardiography. J Am Coll Cardiol 2007;50(20):1981–1989.
15. Petersen SE, Aung N, Sanghvi MM, et al. Reference ranges for cardiac structure and function using cardiovascular magnetic resonance (CMR) in Caucasians from the UK Biobank population cohort. J Cardiovasc Magn Reson 2017;19(1):18.
16. Sörensson P, Heiberg E, Saleh N, et al. Assessment of myocardium at risk with contrast enhanced steady-state free precession cine cardiovascular magnetic resonance compared to single-photon emission computed tomography. J Cardiovasc Magn Reson 2010;12(1):25.
17. Francone M, Carbone I, Agati L, et al. Utility of T2-weighted short-tau inversion recovery (STIR) sequences in cardiac MRI: an overview of clinical applications in ischaemic and non-ischaemic heart disease. Radiol Med (Torino) 2011;116(1):32–46.
18. Bondarenko O, Beek AM, Hofman MB, et al. Standardizing the definition of hyperenhancement in the quantitative assessment of infarct size and myocardial viability using delayed contrast-enhanced CMR. J Cardiovasc Magn Reson 2005;7(2):481–485.
19. Lønborg J, Vejlstrup N, Kelbæk H, et al. Final infarct size measured by cardiovascular magnetic resonance in patients with ST elevation myocardial infarction predicts long-term clinical outcome: an observational study. Eur Heart J Cardiovasc Imaging 2013;14(4):387–395.
20. Bulluck H, Hammond-Haley M, Fontana M, et al. Quantification of both the area-at-risk and acute myocardial infarct size in ST-segment elevation myocardial infarction using T1-mapping. J Cardiovasc Magn Reson 2017;19(1):57.
21. Tavora F, Cresswell N, Li L, Ripple M, Solomon C, Burke A. Comparison of necropsy findings in patients with sarcoidosis dying suddenly from cardiac sarcoidosis versus dying suddenly from other causes. Am J Cardiol 2009;104(4):571–577.
22. Kouranos V, Tzelepis GE, Rapti A, et al. Complementary role of CMR to conventional screening in the diagnosis and prognosis of cardiac sarcoidosis. JACC Cardiovasc Imaging 2017;10(12):1437–1447.
23. Vignaux O, Dhote R, Duboc D, et al. Clinical significance of myocardial magnetic resonance abnormalities in patients with sarcoidosis: a 1-year follow-up study. Chest 2002;122(6):1895–1901.
24. Sgard B, Brillet PY, Bouvry D, et al. Evaluation of FDG PET combined with cardiac MRI for the diagnosis and therapeutic monitoring of cardiac sarcoidosis. Clin Radiol 2019;74(1):81.e9–81.e18.
25. Ma Y, Gal A, Koss MN. The pathology of pulmonary sarcoidosis: update. Semin Diagn Pathol 2007;24(3):150–161.
26. Dweck MR, Abgral R, Trivieri MG, et al. Hybrid magnetic resonance imaging and positron emission tomography with fluorodeoxyglucose to diagnose active cardiac sarcoidosis. JACC Cardiovasc Imaging 2018;11(1):94–107.
27. Cheng VY, Slomka PJ, Ahlen M, Thomson LE, Waxman AD, Berman DS. Impact of carbohydrate restriction with and without fatty acid loading on

myocardial 18F-FDG uptake during PET: a randomized controlled trial. J Nucl Cardiol 2010;17(2):286–291.
28. Lu Y, Grant C, Xie K, Sweiss NJ. Suppression of myocardial 18F-FDG uptake through prolonged high-fat, high-protein, and very-low-carbohydrate diet before FDG-PET/CT for evaluation of patients with suspected cardiac sarcoidosis. Clin Nucl Med 2017;42(2):88–94.
29. Chareonthaitawee P, Beanlands RS, Chen W, et al. Joint SNMMI-ASNC expert consensus document on the role of 18F-FDG PET/CT in cardiac sarcoid detection and therapy monitoring. J Nucl Med 2017;58(8):1341–1353.
30. Osborne MT, Hulten EA, Singh A, et al. Reduction in 18F-fluorodeoxyglucose uptake on serial cardiac positron emission tomography is associated with improved left ventricular ejection fraction in patients with cardiac sarcoidosis. J Nucl Cardiol 2014;21(1):166–174.
31. Ahmadian A, Pawar S, Govender P, Berman J, Ruberg FL, Miller EJ. The response of FDG uptake to immunosuppressive treatment on FDG PET/CT imaging for cardiac sarcoidosis. J Nucl Cardiol 2017;24(2):413–424.
32. Ibrahim T, Bülow HP, Hackl T, et al. Diagnostic value of contrast-enhanced magnetic resonance imaging and single-photon emission computed tomography for detection of myocardial necrosis early after acute myocardial infarction. J Am Coll Cardiol 2007;49(2):208–216.
33. Wisenberg G, Thiessen JD, Pavlovsky W, Butler J, Wilk B, Prato FS. Same day comparison of PET/CT and PET/MR in patients with cardiac sarcoidosis. J Nucl Cardiol doi: 10.1007/s12350-018-01578-8. Published online January 2, 2019.
34. Camici PG, Prasad SK, Rimoldi OE. Stunning, hibernation, and assessment of myocardial viability. Circulation 2008;117(1):103–114.
35. Matoh F, Satoh H, Shiraki K, et al. The usefulness of delayed enhancement magnetic resonance imaging for diagnosis and evaluation of cardiac function in patients with cardiac sarcoidosis. J Cardiol 2008;51(3):179–188.
36. Puntmann VO, Isted A, Hinojar R, Foote L, Carr-White G, Nagel E. T1 and T2 mapping in recognition of early cardiac involvement in systemic sarcoidosis. Radiology 2017;285(1):63–72.
37. Hanneman K, Kadoch M, Guo HH, et al. Initial experience with simultaneous 18F-FDG PET/MRI in the evaluation of cardiac sarcoidosis and myocarditis. Clin Nucl Med 2017;42(7):e328–e334.